A Delta-Operator Technique for Pay-Load Estimation of a 2DOF Flexible Link Robot

M. Rostgaard*, N.K. Poulsen*, O. Ravn◇

*Informatics and Mathematical Modelling,
Building 321, Richard Petersens Plads,
Technical University of Denmark,
DK-2800 Kgs. Lyngby, Denmark.
mrj, nkp@imm.dtu.dk www.imm.dtu.dk/~nkp

◇Automation, Ørsted •DTU ,
Building 326, Elektrovej
Technical University of Denmark,
DK-2800 Kgs. Lyngby, Denmark.
or@iau.dtu.dk www.iau.dtu.dk/~or

IMM Technical Report

2002-02-12 10.57

Abstract

The paper presents a new method for online identification of pay-loads for a two-link flexible robot. The method benefits from the close correspondance between parameters of a discrete-time model represented by means of the Delta-Operator, and those of the underlying continuous-time model. Although the applied principle might be general in nature, the paper is applied to the well-known problem of identifying a pay-load of a moving flexible robot. This problem is almost impossible to solve by measurements, so an estimation technique must be applied. The presented method benefits from the close correspondance with the continuous-time representation to allow a scalar and implicit adaptive technique which based on flexibility measurements leads to the online estimation of the pay-load.

Keywords : *Flexible Link Robot; Delta-Operator; System Identification; Parameter Estimation; Adaptive Control.*

1 Introduction

The desire for high-performance manipulators and the benefits offered by a light-weight flexible arm capable of maneuvering large pay-loads have lead to analysis of the behavior of the dynamics in which flexibility is the essential issue. The high-performance requirements will inevitably produce designs that during operation will excite vibrations in the manipulator structure.

The flexibility generates a severe problem in controlling the motion due to the inevitably excitation of structural vibrations which affect the accuracy of the manipulator. Therefore a successful controller implementation of a flexible manipulator system is contingent on achieving acceptable performance taking into account variations in e.g. pay-load and environmental disturbances.

The aim of the controller is to suppress the structural vibration while in addition to minimize the cycle time of the manipulator system. For flexible manipulator systems, it is necessary to use a model-based controller in order to mitigate the first harmonics. However, changes in pay-load degrades the model and consequently the performance of the control system, unless some sort of adaptation or gain-scheduling is taken into account to estimate these effects.

In order to investigate different aspects of control of flexible links robot configurations an experimental setup has been made. This experimental setup form the basis for the work described in this paper and consists of two very flexible links with two actuators located in the joints. In this work the links are moving in the horizontal plane making gravity ignorable. The geometry of the links makes the predominant bending take place in this plane making it possible to ignore torsion. The actuators are DC-motors with a sufficient gear ratio and tachometers making an analog velocity feedback feasible, this suppresses the friction and other non-linearities in the actuators. Apart from the tachometers there are two kinds of sensors on the setup, a potentiometer in each joint enabling a measurement of the position of the joint and a number of strain gauges located on each link enabling the measurement of the bending of the link. The simulation model used in this study is derived using physical modelling from the this setup. A photograph of the setup is shown in Figure 1 and a schematic view in Figure 3.

In (M'Saad, Dugard & Hammad 1993) experiments are described for a flexible single-beam system, where time-varying black-box input-output forms are proposed as suitable descriptions of the system. In (Luca & Panzieri 1994) experimental results featuring gravity compensation are presented for a double link robot with a flexible forearm. But like other references, practical algorithms seem to igonore the fact that one could construct an adaptation technique that directly gains insight to the pay-load parameter.

This is topic for the present work. By deducting a linear state-space model describing the pay-load parameter's influence in the continuous-time model, it is possible to apply a Delta-Operator technique for estimation of this parameter in discrete-time.

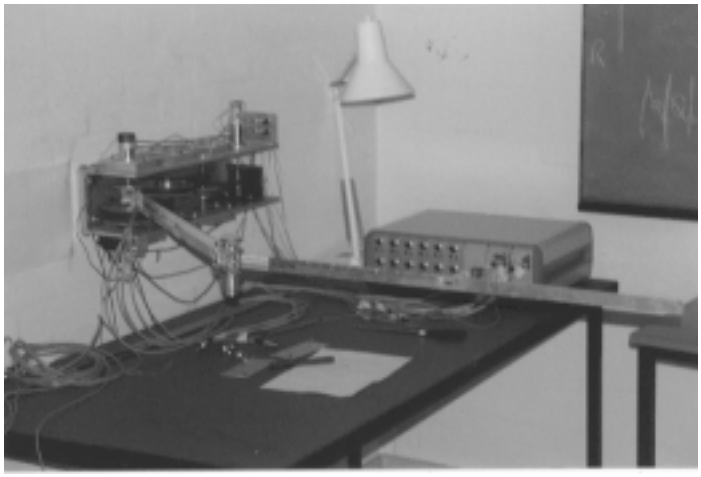

Figure 1. The robot consists of two flexible links and two actuators (DC-motors). It is equipped with two tachometers and four strain gauges in order to measure the link angles and deflection, respectively

To demonstrate this, the paper starts by recapturing the fundamental equations of a two link manipulator system in Section 2. In Section 2.1 the Delta-Operator is introduced, and also the discrete-time estimation technique is presented. As the linearised model is in general sufficient to capture the dynamics of each flexible link, it is demonstrated in Section 4, that the pay-load may be estimated using a recursive parameter estimation technique.

It is worth noting that the presented estimation technique is tied to the Delta-Operator. Provided the discretizing had been based on the conventional shift-operator, one would inevitably had lost the clear physical interpretation of the parameters, and the method would have failed. However, as the presented method is discretised using the Delta-Operator (Middleton & Goodwin 1990), a close correspondence appear between the discrete-time parameters and the underlying continuous-time system.

2 System model

The flexible manipulator system studied here, see Fig. 3, carries a pay-load, m_p, at its tip and moves in the horizontal plane. The active degrees of freedom are the two rotational angles θ_{b1} and θ_2.

In literature the equations of motions are commonly modelled by either a Finite Element Method (see. e.g. (Sakawa, Matsuno & Fukushima 1985)) or the Eigenvalue Method (see e.g. (Kruise 1990)). As the latter method is normally considered more accurate when only a limited number of modes are included, c.f (Baungaard 1996), the following description is be based on this approach, cf. (Rostgaard 1995).

The model of the flexible link robot consists of four parts; namely the models for the two actuators and the two arms. The dynamics of the flexible arms can be

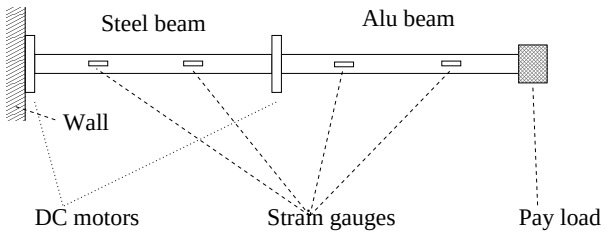

Figure 2. The robot system consists of two flexible links, two actuators (DC motors) and four strain gauges for meaurering the deflection of the links.

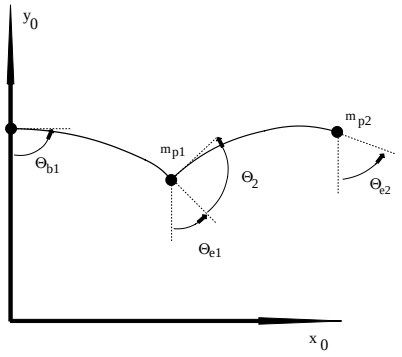

Figure 3. Top view of robot system.

described by a PDE which can be transfered into a ODE by using the method of separation of variable. In that case the deflection, $w_j(x,t), \quad j = 1,2$, of the arms is written as

$$w_j(x,t) = \sum_{i=1}^{\infty} \varphi_{ji}(x) q_{ij}(t)$$

where $\varphi_{ji}(x)$ and $q_{ji}(t)$ are the normal and harmonic function of mode i and arm j, respectively.

2.1 The Main Equations of Motion

For the actuator dynamics, only the first order integration is included, as the time constant of the motor dynamics is typically 10-20 times lower than the first hamonic of the manipulator links. In literature, this has been referred-to as a reduced order of the manipulator system, and this description is attractive from a control point of view, as the reduction affects only the highfrequent area of the actuator dynamics, which is outside the dominant frequency of the structural vibration and thus difficult to observe and control anyhow.

The four basic differential equations can be summarized, cf. (Rostgaard 1995). For the shoulder-actuator:

$$k_{13}\dot{\theta}_{b1} + k_{11}u_1 + k_{12}EI_1 \sum_{i=1}^{n} \varphi_{1i}(0)'' q_{1i} = 0 \tag{1}$$

where k_{11}, k_{12} and k_{13} are parameters descriping actuator 1 and where I_1 is the beam inertia for the upper arm $j = 1$. E is the Young's modulus for the beam.

For the elbow-actuator we have in a similar fashion:

$$k_{23}\dot{\theta}_2 + k_{21}u_2 + k_{22}EI_2\sum_{i=1}^{n}\varphi_{2i}(0)''q_{2i} = 0 \tag{2}$$

For the lower arm (ie. $j = 2$) we have the ODE equation for each mode ($i = 1, 2, \ ... \ n$):

$$\omega_{2i}^2 q_{2i} + 2\zeta_{2i}\omega_{2i}\dot{q}_{2i} + \ddot{q}_{2i} \ = \tag{3}$$

$$\sum_{j=1}^{n}\kappa_{2ij}^*\ddot{q}_{2j} + \alpha_{2i}^*\left[\ddot{\theta}_2 + \ddot{\theta}_{b1} + \sum_{j=1}^{n}\varphi_{1j}'(L_1)\ddot{q}_{1j}(t)\right]$$

$$+\beta_{2i}^*\left[L_1\ddot{\theta}_{b1} + \sum_{j=1}^{n}\varphi_{1j}(L_1)\ddot{q}_{1j}\right]\cos(\theta_2) \tag{4}$$

where ω_{2i} and ζ_{2i} are the harmonic frequency and damping for mode i (and the second or lower arm). L_j is the length of arm j and the modal parameters for the lower arm are linearly denpending of the payload, ie.

$$\begin{aligned}
\alpha_{2i}^* &= \alpha_{2i} - \frac{m_p}{\mu_2}L_2\varphi_{2i}(L) \\
\beta_{2i}^* &= \beta_{2i} - \frac{m_p}{\mu_2}\varphi_{2i}(L_2) \\
\kappa_{2ij}^* &= -\frac{m_p}{\mu_2}\varphi_{2i}(L_2)\varphi_{2j}(L_2)
\end{aligned} \tag{5}$$

where payload free modal parameters, α_{2i} and β_{2i}, are depending on the geometry and the normal functions. μ_2 is one quarter of the mass of the link, ie. $\mu_2 = \frac{1}{4}m_{l2}$.

For the upper arm the situation becomes a little more complicated. This is due to the coupling between elbow-actuator and the deflection of the upper arm. Here the modal equations are:

$$\begin{aligned}
\omega_{1i}^2 q_{1i} + 2\zeta_{1i}\omega_{1i}\dot{q}_{1i} + \ddot{q}_{1i} \ &= \ \sum_{j=1}^{n}\kappa_{1ij}^*\ddot{q}_{1j} + \ddot{\theta}_{b1}\left[\alpha_{1i}^* + \frac{J_h\varphi_{1i}'(L_1)}{\mu_1}\right] \\
&+\frac{J_h\varphi_{1i}'(L_1)}{\mu_1}\sum_{j=1}^{n}\varphi_{1j}'(L_1)\ddot{q}_{1j} - \frac{F_{ye}^{(1)}}{\mu_1}\varphi_{1i}(L_1) \\
&+\frac{J_2\, N_2\varphi_{1i}'(L_1)}{\mu_1}\left[k_{21}u_2 + k_{23}\dot{\theta}_2\right]
\end{aligned} \tag{6}$$

where J_h, J_2 are hub and rotor inertia of actuator 2 and where

$$F_{ye}^{(1)} \ = \ F_{b2}\cos(\theta_2) + F_{x2}\sin(\theta_2)$$

$$
\begin{aligned}
F_{b2} &= EI_2 \sum_{j=1}^{n} \varphi_{2j}(0)''' q_{2j}(t) \\
F_{x2} &= (m_{l2} + m_p)\sin(\theta_2)\left[L_1 \ddot{\theta}_{b1} + \sum_{j=1}^{n} \varphi_{1j}(L)\ddot{q}_{1j}(t) \right]
\end{aligned} \tag{7}
$$

m_{l2} is mass of arm 2. Here the modal parameters α^*_{1i} and β^*_{1i} are independent of the payload mass (but do depend on the mass of actuator 2). Notice, the linear dependence on the pay load mass, m_p, enters through (7).

If the actuator equations, (1) and (2), are used for obtaining the angular accelerations in (4) and (6) the four main equations can be written in a more compact form.

Introduce the notation:

$$
\underline{q} = \left[\; q_{11}, \; \cdots \; q_{1n}, \; q_{21}, \; \cdots \; q_{2n} \; \right]^T, \tag{8}
$$

$$
u = \begin{bmatrix} u_1 \\ u_2 \end{bmatrix}, \quad \underline{\theta} = \begin{bmatrix} \theta_{b1} \\ \theta_2 \end{bmatrix} \tag{9}
$$

Then the description of the flexibility, (4) and (6), can be linearized and brought into the following compact form (see Appendix A, (58)):

$$
\ddot{\underline{q}} = M_1 \underline{q} + M_2 \dot{\underline{q}} + M_3 \ddot{\underline{q}} + M_4 \underline{u} + M_5 \dot{\underline{u}} \tag{10}
$$

where the matrices, M_2, M_3 and M_5 are affine in m_p. Notice, the matrices depend on the linearization point. In this case the matrices depend only on θ_2. Also, notice the angular acceleration, $\underline{q}$, occurs on both side of the i equation.

Also the actuator dynamics can be written in a compact form (see Appendix A, (60))

$$
\dot{\theta} = M_6 \underline{q} + M_7 u \tag{11}
$$

Now the compact description in (10) and (11) is to be transformed into a state space description. The algebraic loop (related to $\ddot{\underline{q}}$ in (10)) can be solved if the following matrix inverse exists,

$$
\Lambda = (I - M_3)^{-1}
$$

Notice M_3 depend linearly on the pay load mass, m_p. Taking the states

$$
x = \begin{bmatrix} \underline{\theta} \\ \underline{q} \\ \dot{\underline{q}} - \Lambda M_5 u \end{bmatrix} \tag{12}
$$

one obtains easily the state space description

$$
\dot{x} = \underbrace{\begin{bmatrix} 0 & M_6 & 0 \\ 0 & 0 & I \\ 0 & \Lambda M_1 & \Lambda M_2 \end{bmatrix}}_{\underline{A}} x + \underbrace{\begin{bmatrix} M_7 \\ \Lambda M_5 \\ \Lambda M_2 \Lambda M_5 + \Lambda M_4 \end{bmatrix}}_{\underline{B}} u
$$

where the state transition matrix is of order $2 + 4n$ with n as the number of considered modes. For an arbitrary linearization angle, this representation is a linear approximation to the dynamics, i.e. M_i are functions of the linearization angle. Thus, one can use the measurements of θ_2 to obtain a running linear description around the actual orientation.

Since the pay load mass is unknown or even time varying we will have rephrase the model in such a way that it is possible to estimate the pay load mass, m_p. The suggested method takes starting point in the split-up of the state transition and state control matrices of the form

$$\underline{A} = \underline{A}^0 + m_p \underline{A}^m, \quad \underline{B} = \underline{B}^0 + m_p \underline{B}^m \tag{13}$$

where m_p is the pay-load attached to the lower arm. It is to be preferred that the four matrices on the right hand side are mass independent. Since, it is the M_i matrices, which are linearly dependent on m_p, this is however not the case. This leads to a pseudo-linear description where the four state space matrices in (13) depend on m_p. This might be seen as a problem, but the method proposed in this paper, is based on recursive estimation of m_p. That opens for the possibility of using the a priory estimate of m_p in the expressions for the four state space matrices in (13).

We have in the previous sections established the following linear dependencies of m_p

$$\begin{aligned} M_2 &= M_2^0 + m_p M_2^m \\ M_3 &= M_3^0 + m_p M_3^m \\ M_5 &= M_5^0 + m_p M_5^m \end{aligned} \tag{14}$$

while M_1, M_4, M_6 and M_7 are independent of m_p. Notice (13) is not necessarily a Taylor expansion, but heavily rely on the definition of the four matrices in (13). If we define:

$$\begin{aligned} \underline{A}^0 &= \begin{bmatrix} 0 & M_6 & 0 \\ 0 & 0 & I \\ 0 & \Lambda M_1 & \Lambda M_2^0 \end{bmatrix} \qquad \underline{A}^m = \begin{bmatrix} 0 & 0 & 0 \\ 0 & 0 & 0 \\ 0 & 0 & \Lambda M_2^m \end{bmatrix} \\ \underline{B}^0 &= \begin{bmatrix} M_7 \\ \Lambda M_5 \\ \underline{B}_3^0 \end{bmatrix} \qquad \underline{B}^m = \begin{bmatrix} 0 \\ \Lambda M_5^m \\ \Lambda M_2^m \Lambda M_5^0 + \Lambda M_2^0 \Lambda M_5^m \end{bmatrix} \end{aligned} \tag{15}$$

where

$$\underline{B}_3^0 = \Lambda M_2^0 \Lambda M_5^0 + m_p^2 \Lambda M_2^m \Lambda M_5^m + \Lambda M_4 \tag{16}$$

then (13) is fulfilled.

3 The measurement system

The measurement system consists of two tachometers and four strain gauges. The tachometers give measurements of the link angles θ_{b1} and θ_2, whereas the

strain gauges are located tactically on the links in order to give measurements of the deflections ie. $\underline{q}$.

The measurement are connected to the state of the description through

$$y_t = Cx_t \quad C = \begin{bmatrix} C_{tg} & 0 & 0 \\ 0 & C_{sg1} & 0 \\ 0 & 0 & C_{sg2} \end{bmatrix} \tag{17}$$

where C_{tg}, C_{sg1} and C_{sg2} are observation matrices for the two tachometers and the strain gauges located on the two links. These are:

$$C_{tg} = \begin{bmatrix} k_{tg1} & 0 \\ 0 & k_{tg2} \end{bmatrix} \qquad C_{sg1} = \begin{bmatrix} k_{sg1}\varphi''_{11}(l_{11}) & k_{sg1}\varphi''_{12}(l_{11}) \\ k_{sg2}\varphi''_{11}(l_{12}) & k_{sg2}\varphi''_{12}(l_{12}) \end{bmatrix}$$

(C_{sg2} is defined in a similar manner). The constants k_{tgi} and k_{sgi} are constants characterizing the tachometers and the strain gauge, whereas l_{ji} are the location (no i) on the the links (link no. j).

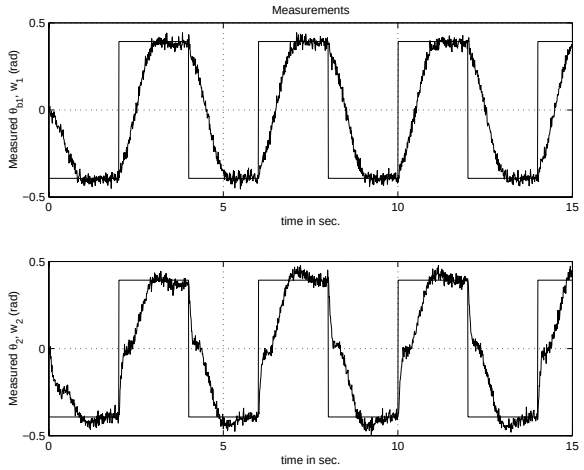

Figure 4. Measuremed angles θ_{b1} and θ_2 and their reference w_1 and w_2.

4 The pay-load estimation

So far the model of the dynamics has been given in the continuous-time form

$$\begin{aligned} \underline{A} &= \underline{A}^0 + m_p(t)\,\underline{A}^m \\ \underline{B} &= \underline{B}^0 + m_p(t)\,\underline{B}^m \end{aligned} \tag{18}$$

where the four matrices on the right hand side are calculated based on information available at time $t-1$. The system is sampled with a period of T. By use of the approximation

$$\begin{aligned} \Omega &= \frac{1}{T}\int_0^T e^{(\,\underline{A}^0 + m_p(t-1)\,\underline{A}^m\,)\,\tau} d\tau \\ &\approx I + \sum_{i=1}^{n'} \frac{((\underline{A}^0 + m_p(t-1)\,\underline{A}^m)\,T)^i}{(i+1)!} \end{aligned} \tag{19}$$

(n' being "large"), the discrete-time delta-model shows a similar linearity of the pay-load as its continuous-time counterpart,

$$\begin{aligned} \overline{A}^0 &= \Omega\,\underline{A}^0, \qquad \overline{B}^0 = \Omega\,\underline{B}^0 \\ \overline{A}^m &= \Omega\,\underline{A}^m, \qquad \overline{B}^m = \Omega\,\underline{B}^m \end{aligned} \tag{20}$$

Obviously, as m_p tends to stationarity the approximation becomes better. If $m_p(t-1) = m_p(t)$ then the discrete-time model

$$\begin{aligned} \delta x_t &= \overline{A} x_t + \overline{B} u_t \\ y_t &= \overline{C} x_t \end{aligned} \tag{21}$$

using the definitions

$$\begin{aligned} \overline{A} &= \overline{A}^0 + m_p(t)\,\overline{A}^m \\ \overline{B} &= \overline{B}^0 + m_p(t)\,\overline{B}^m \end{aligned} \tag{22}$$

describes perfectly the underlying continuous-time system at the sampling instants.

4.1 Adaptation of the pay-load

In general (21) is connected with a Kalman predictor ($\overline{K}$, $\overline{P}$) that takes into account measurements

$$\delta\hat{x}_t = \overline{A}\hat{x}_t + \overline{B}u_t + \overline{K}(y_t - \overline{C}\hat{x}_t) \tag{23}$$

This estimate can be put into a linear mass-dependent form

$$\hat{x}_t = \hat{x}_t^0 + m_p(t)\,\hat{x}_t^m \tag{24}$$

Here

$$\begin{aligned} \hat{x}_t^0 &= (I + T\,\overline{A}^0 - T\,\overline{K}\,\overline{C})\,\hat{x}_{t-1} \\ &\quad + T\,\overline{B}^0 u_{t-1} + T\,\overline{K}\,y_{t-1} \\ \hat{x}_t^m &= T\,\overline{A}^m\,\hat{x}_{t-1} + T\,\overline{B}^m\,u_{t-1} \end{aligned} \tag{25}$$

and $\overline{A}$, $\overline{B}$, $\overline{C}$ and $\overline{K}$ are all calculated on the basis of information available at time $t-1$. In particular $\overline{C}$ does not have to be a row vector. Therefore all measurements are used to construct the best estimates of $\hat{x}_t$ and consequently also of $\hat{x}_t^0$ and $\hat{x}_t^m$. In contrast to this, let

$$y_t' = \overline{C}'\,\hat{x}_t + e_t \tag{26}$$

be a single composite measurement (possibly a weighted sum of all measurements) and $\overline{C}'$ a row vector (with entries that correspond to the composite measurement). The noise term e_t is zero-mean and uncorrelated with $\hat{x}_t$. From (24) and (26) the least squares regression model

$$\psi_t = \varphi_t^\top\,\theta_t + e_t \tag{27}$$

is produced with

$$\begin{aligned} \psi_t &= y'_t - \overline{C}'\,\hat{x}_t^0 \\ \varphi_t^\top &= \overline{C}'\hat{x}_t^m \\ \theta_t &= m_p(t) \end{aligned} \tag{28}$$

The regression form is pseudo-linear since φ_t is calculated on the basis of the estimate at time $t-1$. However, by use of this approach all measurements are used to construct the "best" estimate of $\hat{x}_t$, although only a single composite measurement is used within the regression part. This will possibly imply a better estimate asymptotically, since the additional measurements will guide the model in the direction of the true plant model (if plant model is within the model set). The choice of y'_t is here taken in an ad-hoc way as the angle of the end-point of the forearm, θ_{2e}. This choice seems reasonable since the lower arm is mostly affected by variations in the pay-load.

To obtain a robust parameter identification a selective forgetting method is suggested, (Parkum 1992). This algorithm shows tracking ability without the drawback of covariance blow-up. The method has a close parallel to the EFRA method and gains the same advantages at a less computational expense. This overcomes the problems of neither the covariance matrix tending to zero nor to blow-up. Also it guarantees that identification is always alert to some extent. The selective forgetting scheme (SF1) can be written as

$$\begin{aligned} \epsilon_t &= \psi_t - \varphi_t^\top \hat{\theta}_{t-1} \\ \kappa_t &= \frac{P_{t-1}\varphi_t}{1+\varphi_t^\top P_{t-1}\varphi_t} \\ \hat{\theta}_t &= \hat{\theta}_{t-1} + \kappa_t \epsilon_t \\ P_{t|t-1} &= \frac{\alpha_1-\alpha_0}{\alpha_1} P_{t-1} + \alpha_0 I \\ P_t &= (I - \kappa_t \varphi_t^\top)\, P_{t|t-1} \end{aligned} \tag{29}$$

where $0 < \alpha_0 < \alpha_1 < \infty$. The algorithm is illustrated in Fig. 5 - Fig. 9 using the parameters:

$$\begin{array}{lll} \alpha_0 = 0.1, & \alpha_1 = 2, & P_0 = 2 \\ \hat{\theta}_0 = 0, & m_p = 0.1, & T = 0.01 \\ n' = 15 & R_1 = 10^{-4}\, I & R_2 = 10^{-4}\, I \end{array} \tag{30}$$

where R_1, R_2 denote respectively the process and the measurement covariance matrices. The state space LQG controller is iterated a single iteration per sample — asymptotically producing the optimal feed-back gain based on the loss covariances

$$Q_1 = \overline{C}'^{\top}\overline{C}', \quad Q_2 = 0.005\, I \tag{31}$$

The value of m_p can be compared to e.g. the mass of the lower arm, $m_{l2} = 0.133$, saying that the manipulator is heavily loaded. A better performance can be seen after the second step reflecting that m_p is almost estimated after 3 seconds, see Fig. 5. From here it also appears that only when the set-points are varied new information is obtained.

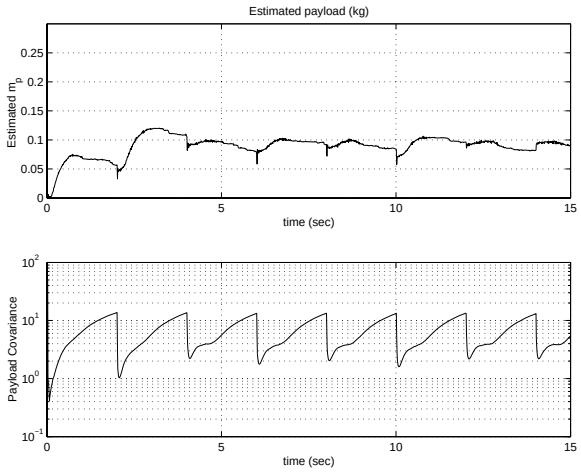

Figure 5. Estimated pay-load $\hat{m}_p(t)$ and variance of estimate in a closed-loop experiment.

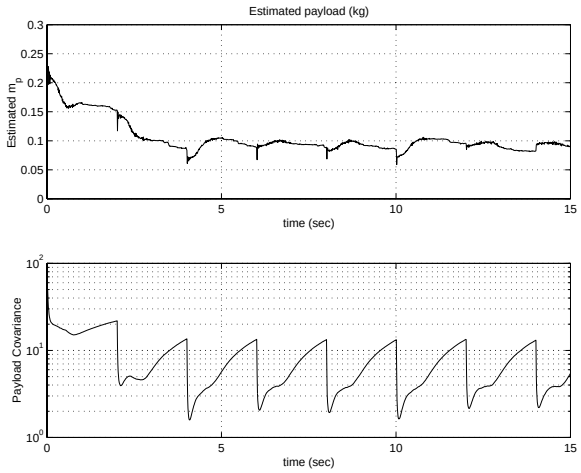

Figure 6. Estimated pay-load $\hat{m}_p(t)$ and variance of estimate in a closed-loop experiment.

5 Conclusions

The paper has presented a new method for online identification of pay-loads for a two-link flexible robot. First the state-space model has been derived, and then the model is discretised using the Delta-Operator, which benefits from the close correspondance between parameters of a discrete-time model and those of the underlying continuous-time model. Due to the close correspondance, it is shown that both domain models can produce almost the same linearity with respect to a pay-load. This fact is used in a pay-load estimation technique. By simulation it is demonstrated that it is possible to identify a time-varying pay-load of a two link flexible robot during closed-loop control.

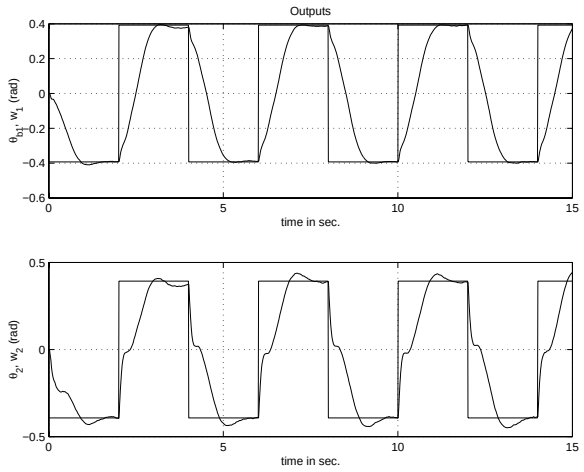

Figure 7. Angular positions θ_{b1} and θ_2 presented as measured outputs '__' and as reference trajectories '_._.'.

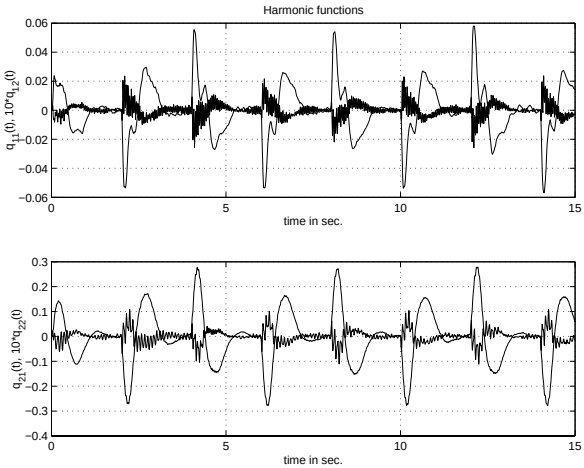

Figure 8. Harmonic time-functions q_{i1} and $10\,q_{i2}$ for each of the beams, $i = 1, 2$ presented as functions of time.

6 Acknowledgement

This research was gratefully supported by a grant from the Danish Research Council for Technical Science, STVF (Statens Teknisk-Videnskabelige Forskningsråd) under license no. 16-5059.

A Dynamics of a DC motor

Consider a DC motor, which (cf. (Leth 1982)) can be described (to a reasonable desgree) by a first order model as depicted in Figure 10. Let V_a denote the voltage input, M_m is the resulting external torque (ie. torque not included in the model) and $\dot{\theta}_m$ is the angular velocity of the motor shaft. Then using

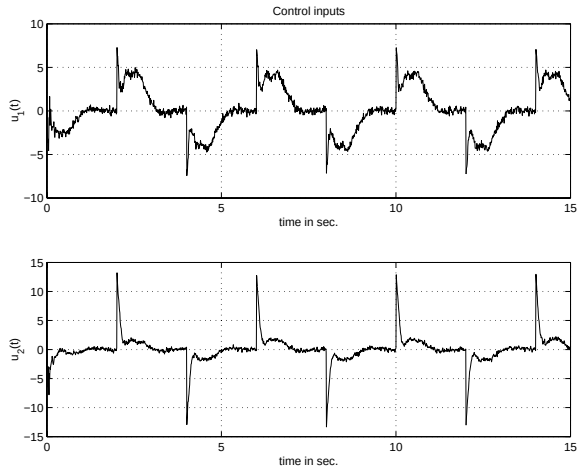

Figure 9. Control inputs u_1 and u_2 as functions of time.

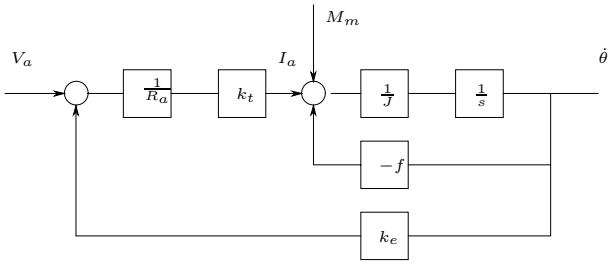

Figure 10. DC-motor

Newton second law the mode can given as

$$J\ddot{\theta}_m = M_m - f\dot{\theta}_m + \frac{k_t}{R_a}\left(V_a - k_e\dot{\theta}_m\right)$$

where $k_e = k_t$ represent motor constants, f the total viscous friction of the motor, R_a the electrical resistance and J the total inertia of motor. Introducing the dynamic constants

$$F = \frac{k_e k_t}{R_a} \qquad \tau_m = \frac{J}{F+f} \qquad k_{vm} = \frac{k_t}{R_a(F+f)} = \frac{k_t}{k_e k_t + f R_a}$$

$$\tau_m\ddot{\theta}_m + \dot{\theta}_m = k_{vm}V_a + \frac{R_a}{k_t}k_{vm}M_m$$

A.1 Tacho feed back

In order to reduce the influence from the disturbances, non linearities and other imperfects, the DC-motor is included in a tacho loop, in which the difference

between the reference voltage V_r and the tacho voltage $V_{tg} = k_{tg}\dot{\theta}_m$ is amplified (gain k_p) and feed into the motor, ie.

$$V_a = k_p(V_r - k_{tg}\dot{\theta}_m)$$

input voltage is

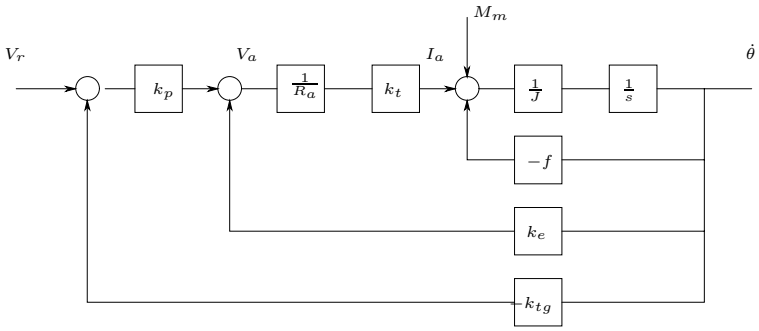

Figure 11. DC-motor

If for short

$$k_{et} = k_e + k_p k_{tg} \qquad F_t = \frac{k_{et}k_t}{R_a}$$

the Newtons second law gives the description

$$J\ddot{\theta}_m + (f + F_t)\dot{\theta}_m = \frac{k_t k_p}{R_a}V_r + \frac{1}{f + F_t}M_m$$

or

$$\tau_{mt}\ddot{\theta}_m + \dot{\theta}_m = k_p k_{vmt}V_r + \frac{R_a}{k_t}k_{vmt}M_m$$

where

$$\tau_{mt} = \frac{J}{f + F_t}$$

$$k_{vmt} = \frac{k_t}{R_a(f + F_t)} = \frac{k_t}{k_{et}k_t + fR_a} = \frac{k_{vm}}{1 + k_p k_{tg} k_{vm}}$$

A.2 Gear

There is a gear between the motor shaft (θ_m) and the manipulator (θ_b). The gear is considered stiff and is constructed as a three step gear with a total gear-ratio of N,

$$\theta_b = \frac{1}{N}\theta_m$$

Let M_b denote the external momentum affecting the motor at the external shaft, where

$$M_b = NM_m$$

It is convenient to rewrite the motor equation as

$$\ddot{\theta}_b = k_1 V_r + k_2 M_b + k_3 \dot{\theta}_b \tag{32}$$

where the constants are

$$\begin{aligned} k_1 &= \frac{k_{vmt} k_p}{N \tau_{mt}} \\ k_2 &= \frac{k_{vmt} R_a}{N^2 k_t \tau_{mt}} = \frac{1}{JN^2} \\ k_3 &= -\frac{1}{\tau_{mt}} \end{aligned} \tag{33}$$

Let us define

$$J_b = N^2 J$$

then

$$J_b \ddot{\theta}_b = J_b \Big(k_1 V_r + k_3 \dot{\theta}_b \Big) + M_b \tag{34}$$

or from the motor side:

$$J \ddot{\theta}_m = J \Big(N k_1 V_r + k_3 \dot{\theta}_m \Big) + M_m$$

The induced torque is given by

$$\begin{aligned} M_d &= J_b \ddot{\theta}_b - M_b \\ &= J_b \Big(k_1 V_r + k_3 \dot{\theta}_b \Big) \end{aligned} \tag{35}$$

and

$$M_{dm} = J \Big(N k_1 V_r + k_3 \dot{\theta}_m \Big)$$

from the motor side.

B Dynamics of a prismatic beam

Consider the beam segment in Figure 12. Let x denote the distance along the beam and $w(x,t)$ the deflection of the beam. Here a is the cross section area of the beam. The beam is physically described by b, h and L representing the measures width, height and length. Since transversal vibrations appear athwart to the beam the cross section area and inertia are

$$\begin{aligned} a &= b\,h \\ I &= \int_0^h [2 \int_0^{\frac{b}{2}} r^2 dr] dy = \frac{b^3 h}{12} \end{aligned} \tag{36}$$

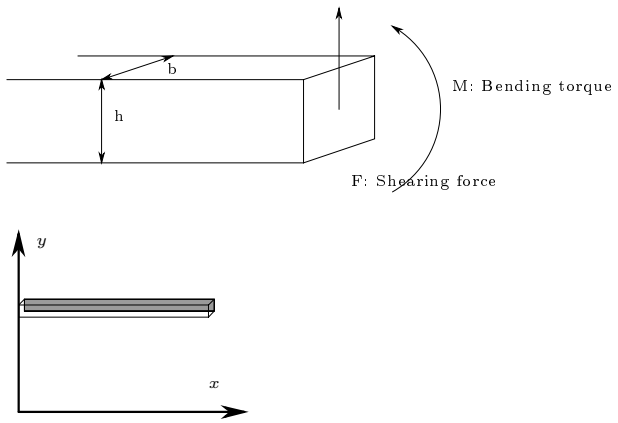

Figure 12. Forces and torque in a cross section of a beam

Taking the resulting shearing forces and torque we obtain the following relations

$$\frac{\partial F}{\partial x} + \rho a \frac{\partial^2 w(x,t)}{\partial t^2} = 0$$

and

$$F = \frac{\partial M}{\partial x}$$

From the elementary flexural theory (Timoshenko, Young & Weaver 1974) we have

$$M = EI \frac{\partial^2 w(x,t)}{\partial x^2}$$

These three last equations gives us the Euler Bernoulli equation for the beam

$$EI \frac{\partial^4 w(x,t)}{\partial x^4} = -\rho a \frac{\partial^2 w(x,t)}{\partial t^2} \tag{37}$$

The solution to this equation with boundary conditions can be found by using separation of variable. This means

$$w(x,t) = \sum_{i=1}^{\infty} \varphi_i(x) q_i(t)$$

which is equivalent of expand the deflection of the beam in modes. $\varphi_i(x)$ represent functions of x that define the shapes of the natural modes of vibration and are called *principal functions* or *normal functions*, (Timoshenko et al. 1974). It can be shown (see (Rostgaard 1995) for details) that the normal functions are orthogonal and posses other interesting properties. $q_i(t)$ describes a harmonic time-function. With this expansion we have

$$M = EI \sum_{i=1}^{\infty} q_i(t) \frac{\partial^2 \varphi_i(x)}{\partial x^2} \qquad F = EI \sum_{i=1}^{\infty} q_i(t) \frac{\partial^3 \varphi_i(x)}{\partial x^3}$$

For each mode we have the following

$$\begin{aligned}\frac{\partial^2 q_i(t)}{\partial t^2} + \omega_i^2 q_i(t) &= 0 \\ \frac{\partial^4 \varphi_i(x)}{\partial x^4} - \gamma_i^4 \varphi_i(x) &= 0\end{aligned}$$

where

$$\omega_i^2 = \frac{EI}{\rho\, a}\gamma_i^4$$

The general solution to the time-function is

$$q_i(t) = A_i\ cos(\omega_i t) + B_i\ sin(\omega_i t)$$

whereas the solution to the normal function can be written as

$$\begin{aligned}\varphi_i(x) &= c_{1i}\cosh(\gamma_i x) + c_{2i}\sinh(\gamma_i x) \\ &\quad + c_{3i}\cos(\gamma_i x) + c_{4i}\sin(\gamma_i x)\end{aligned} \tag{38}$$

It might be useful to notice that

$$\frac{\partial^n \varphi_i(x)}{\partial x^n} = \gamma_i^n\ \ (c_{1i}\ c_{2i}\ c_{3i}\ c_{4i}) \begin{bmatrix} 0 & 1 & 0 & 0 \\ 1 & 0 & 0 & 0 \\ 0 & 0 & 0 & -1 \\ 0 & 0 & 1 & 0 \end{bmatrix}^n \begin{bmatrix} \cosh(\gamma_i x) \\ \sinh(\gamma_i x) \\ \cos(\gamma_i x) \\ \sin(\gamma_i x) \end{bmatrix}$$

B.1 Clamped - free beam

The constants (A_i, B_i, c_{1i}, c_{2i}, c_{3i}, c_{4i}) are determined from the boundary conditions (in time and space). In the clamped - free case we have the following conditions on the normal function

$$\varphi_i(0) = 0 \qquad \frac{\partial \varphi_i(0)}{\partial x} = 0 \qquad \frac{\partial^2 \varphi_i(L)}{\partial x^2} = 0 \qquad \frac{\partial^3 \varphi_i(L)}{\partial x^3} = 0 \tag{39}$$

The first two conditions are due to clamped end ($x = 0$) and the latter are coursed by the fact that $F(L) = 0$ and $M(L) = 0$.

$$\begin{aligned}0 &= c_{1i} + c_{3i} \\ 0 &= \gamma_i(c_{2i} + c_{4i}) \\ 0 &= \gamma_i^2\,(c_{1i}\cosh(\gamma_i L) + c_{2i}\sinh(\gamma_i L) - c_{3i}\cos(\gamma_i L) - c_{4i}\sin(\gamma_i L)) \\ 0 &= \gamma_i^3\,(c_{1i}\sinh(\gamma_i L) + c_{2i}\cosh(\gamma_i L) + c_{3i}\sin(\gamma_i L) - c_{4i}\cos(\gamma_i L))\end{aligned} \tag{40}$$

The only non trivial solution (cf. (Rostgaard 1995), p. 14) to 40 obeys

$$c_{3i} = -c_{1i} \qquad c_{4i} = -c_{2i}$$

and (to ensure a nontrivial solution to the last two equations in (40))

$$\cosh(\gamma_i L)\cos(\gamma_i L) = -1 \tag{41}$$

which is denoted as the *frequency equation*. Its numerical solution is discussed in Appendix G.

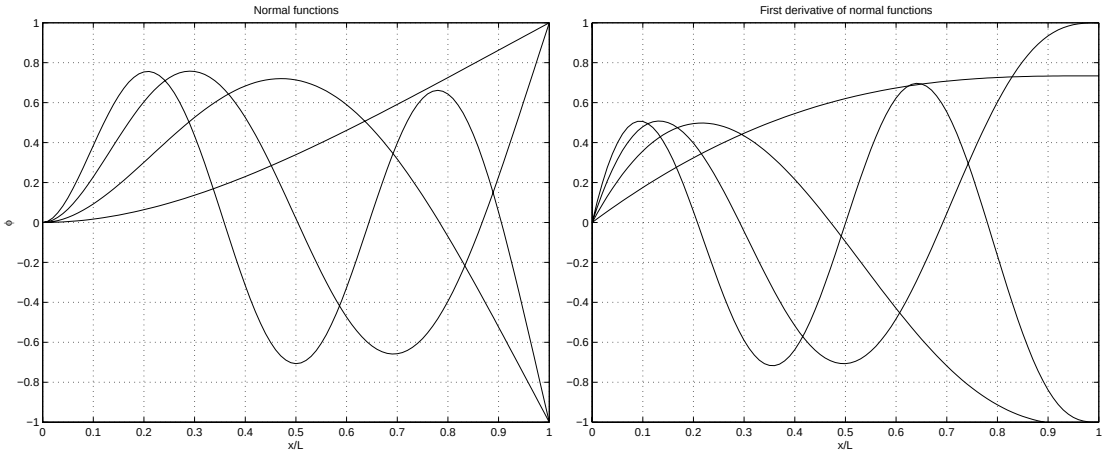

Figure 13. *Normal functions and their first derivative.*

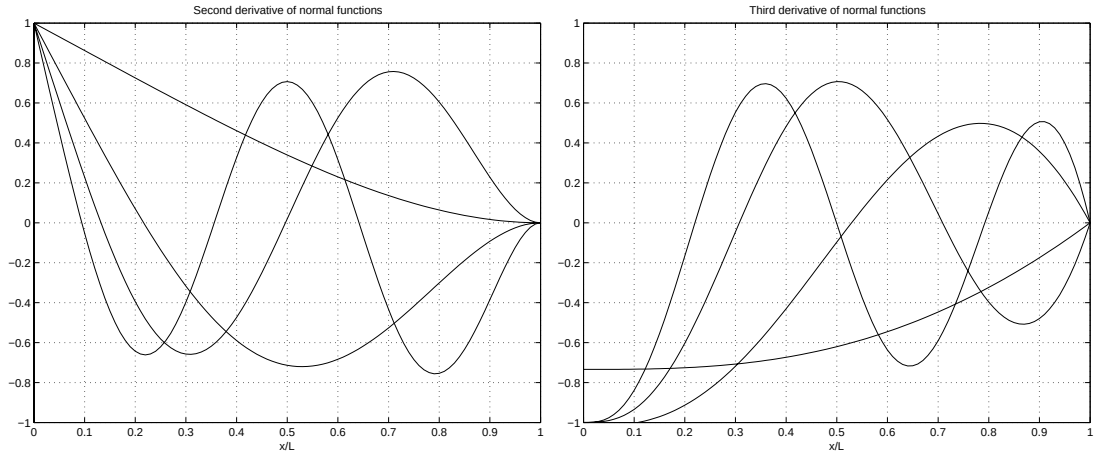

Figure 14. *Second and third derivative of normal functions, which are proportional to torque and shear force.*

C A moving beam with external forces

See (Rostgaard 1995) page 26-28.

Assume that the beam is moving such its beginning having an acceleration, $\ddot{y}_b$, perpendicular to beam axe. The angle between the beam axe and vertical is θ_b. Furthermore, assume that an external force, F_e, perpendicular to the beam axe and a torque is acting at the end of the beam.

In this case, the Euler-Bernoulli equation (37), is extended to

$$\begin{aligned} EI\frac{\partial^4 w(x,t)}{\partial x^4} + \rho a\frac{\partial^2 w(x,t)}{\partial t^2} \\ +\rho a\Big[\ddot{y}_b + x\ddot{\theta}_b + w\dot{\theta}_b + g\sin(\theta_b)\Big] \\ +\frac{\partial \delta(x-L)M_e}{\partial x} + \delta(x-L)F_e = 0 \end{aligned} \tag{42}$$

Using the same method (separation of variable) as in appendix B where the deflection is expanded in modes, ie.

$$w(x,t) + \sum_{i=0}^{\infty} \varphi_i(x) q_i(t)$$

equation (42) becomes

$$\begin{aligned} \omega_i^2 q_i + 2\zeta_i\omega_i\dot{q}_i + \ddot{q}_i \\ = \alpha_i\ddot{\theta}_b + \beta_i\Big[\ddot{y}_b + g\sin(\theta_b)\Big] \\ -\frac{1}{\mu}\frac{\partial\varphi_i(L)}{\partial x}M_e - \frac{\varphi_i(L)}{\mu}F_e \end{aligned} \tag{43}$$

where

$$\alpha_i = -\frac{4}{L}\int_0^L x\varphi_i(x)dx \tag{44}$$

$$\beta_i = -\frac{4}{L}\int_0^L \varphi_i(x)dx \tag{45}$$

$$\mu = \frac{\rho a L}{4}$$

Here the coriolis term $w\dot{\theta}_b$ has been neglected and friction has been added to the model. See appendix H for numerical method for determine the beam constants α_i, β_i and μ.

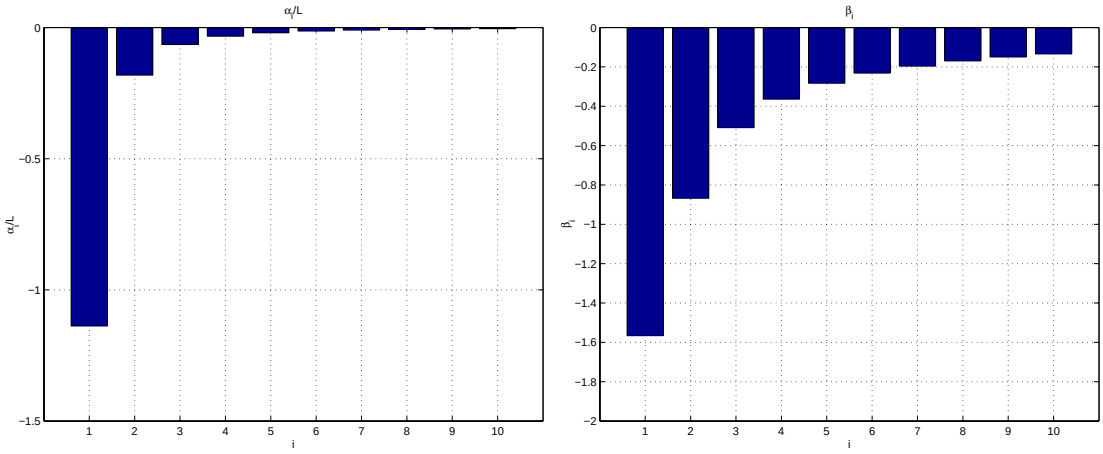

Figure 15. *Plot of α_i/L and β_i*

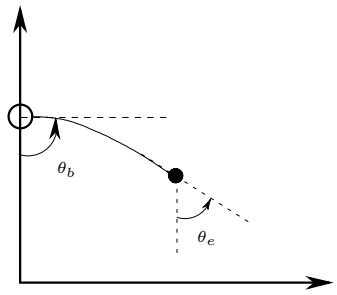

Figure 16. 1DOF flexible robot arm.

D 1DOF flexible link with payload

The link is affected by a mounted DC-motor and a payload (mass m_p) positioned at the end of the beam. Applying Newtons law on the pay load, we have

$$m_p \ddot{y}_e = F_e - m_p g \sin(\theta_b)$$

where the perpendicular accelration of the end point (and the pay load) is

$$\ddot{y}_e = L\ddot{\theta}_b + \ddot{w}(L,t)$$

ie

$$F_e = m_p \Big[l\ddot{\theta}_b + \sum_{j=1}^{\infty} \varphi_j(L)\ddot{q}_j + g\sin(\theta_b) \Big] \tag{46}$$

Assuming $M_e = 0$ (ie. assuming the pay load is a point mass) (43) becomes:

$$\begin{aligned} \omega_i^2 q_i + 2\zeta_i\omega_i\dot{q}_i + \ddot{q}_i = &\Big[\alpha_i - \frac{m_p}{\mu}\varphi_i(L)\Big]\ddot{\theta}_b \\ &+ \Big(\beta_i - \frac{m_p}{\mu}\varphi_i(L)\Big) g\sin(\theta_b) \end{aligned} \tag{47}$$

$$-\frac{m_p}{\mu}\varphi_i(L)\sum_{j=1}^{\infty}\varphi_j(L)$$

This can also be written as

$$\omega_i^2 q_i + 2\zeta_i\omega_i\dot{q}_i + \ddot{q}_i = \alpha_i^\star\ddot{\theta}_b + \beta_i^\star g\sin(\theta_b) + \sum_{j=1}^{\infty}\kappa_{ij}^\star\ddot{q}_j(t)$$

where

$$\begin{aligned}\alpha_i^\star &= \alpha_i - \frac{m_p}{\mu}\varphi_i(L)\\ \beta_i^\star &= \beta_i - \frac{m_p}{\mu}\varphi_i(L)\\ \kappa_{ij}^\star &= -\frac{m_p}{\mu}\varphi_i(L)\varphi_j(L)\end{aligned} \tag{48}$$

The DC-moter is descriped by (32)

$$\ddot{\theta}_b = k_1 V_r + k_2 M_b + k_3\dot{\theta}_b \tag{49}$$

where

$$M_b = EI\sum_{i=1}^{\infty}\varphi_i''(0)q_i(t)$$

D.1 Moving 1DOF with payload and external forces

If the beam with pay load is moving and have external forces the (43) becomes

$$\begin{aligned}\omega_i^2 q_i + 2\zeta_i\omega_i\dot{q}_i + \ddot{q}_i = \alpha_i^\star\ddot{\theta}_b + \beta_i^\star g\sin(\theta_b) + \sum_{j=1}^{\infty}\kappa_{ij}^\star\ddot{q}_j(t)\\ +\beta_i\ddot{y}_b\\ -\frac{1}{\mu}\frac{\partial\varphi_i(L)}{\partial x}M_e - \frac{\varphi_i(L)}{\mu}F_e\end{aligned} \tag{50}$$

where F_e and M_e are external shear forces and torques (in additional to the force from the pay load).

E 2DOF flexible link robot with pay load

E.1 Beam 1

The effect on beam 1 of the actuator 2 is modelled as a pay load. The impact of beam 2 is described through F_{1e} and M_{1e}.

The resulting torque on the end point gives:

$$J_h\ddot{\theta}_{1e} = -M_{1e} - M_d$$

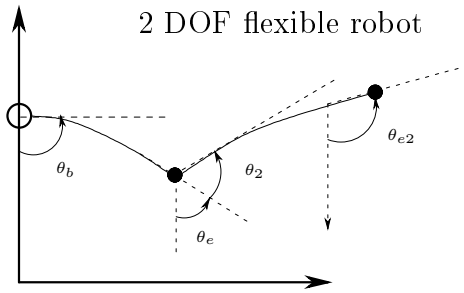

Figure 17. 2DOF flexible robot arm.

where the induced torque (cf. (35)) is given by:

$$M_d = J_2 N_2 \Big(k_{21} u_2 + k_{23} \dot{\theta}_2 \Big)$$

and

$$\ddot{\theta}_{1e} = \ddot{\theta}_1 + \sum_{j=1}^{\infty} \frac{\partial \varphi_{1j}(L)}{\partial x} \ddot{q}_{1j}$$

This results in

$$M_{1e} = -J_h \ddot{\theta}_1 - J_h \sum_{j=1}^{\infty} \frac{\partial \varphi_{1j}(L)}{\partial x} \ddot{q}_{1j} - J_2 N_2 \Big(k_{21} u_2 + k_{23} \dot{\theta}_2 \Big) \tag{51}$$

The shear force acting on the end point is the orthogonal projection of the shear (F_{b2}) and the axial (F_{x2}) force from beam 2, ie.

$$F_{1e} = F_{b2} \cos(\theta_2) - F_{x2} \sin(\theta_2) \tag{52}$$

where

$$F_{b2} = EI_2 \sum_{i-1}^{\infty} \varphi_{2i}'''(0) q_{2i}$$

and

$$F_{x2} = -(m_{l2} + m_p) \ddot{x}_{b2} + ((m_{l2} + m_p) g \cos(\theta_2)$$

where

$$\begin{aligned} \ddot{x}_{b2} &= \ddot{y}_{e1} \sin(\theta_2) \\ &= \Big(L_1 \ddot{\theta}_{b1} + \sum_{i=1}^{\infty} \varphi_{1i}(L) \ddot{q}_{1i} \Big) \sin(\theta_2) \end{aligned} \tag{53}$$

Introducing this in (50) we are obtaining (6) and (37) ie..

$$\begin{aligned} \omega_{1i}^2 q_{1i} + 2\zeta_{1i}\omega_{1i}\dot{q}_{1i} + \ddot{q}_{1i} &= \sum_{j=1}^{n} \kappa_{1ij}^* \ddot{q}_{1j} + \ddot{\theta}_{b1} \left[\alpha_{1i}^* + \frac{J_h \varphi_{1i}'(L_1)}{\mu_1} \right] \\ &+ \frac{J_h \varphi_{1i}'(L_1)}{\mu_1} \sum_{j=1}^{n} \varphi_{1j}'(L_1) \ddot{q}_{1j} - \frac{F_{ye}^{(1)}}{\mu_1} \varphi_{1i}(L_1) \\ &+ \frac{J_2 \, N_2 \varphi_{1i}'(L_1)}{\mu_1} \Big[k_{21} u_2 + k_{23} \dot{\theta}_2 \Big] \end{aligned}$$

and

$$\begin{aligned} F_{ye}^{(1)} &= F_{b2}\cos(\theta_2) + F_{x2}\sin(\theta_2) \\ F_{b2} &= EI_2 \sum_{j=1}^{n} \varphi_{2j}(0)''' q_{2j}(t) \\ F_{x2} &= (m_{l2}+m_p)\left[L_1\ddot{\theta}_{b1}\sin(\theta_2) + \sum_{j=1}^{n} \varphi_{1j}(L)\ddot{q}_{1j}(t)\sin(\theta_2) \right] \end{aligned}$$

E.2 Beam 2

For the lower beam (beam 2) there are no external forces (except for the effect from the pay load), so the only non zero terms in (50) are the accelrations of the beginning of the beam (ie. $\ddot{y}_{b2}$ and $\ddot{\theta}_{b2}$).

Now, since

$$\theta_{b_2} = \theta_1 + \sum_{i=1}^{\infty} \varphi'_{1i}(L) q_{1i} + \theta_2$$

the angular accelration is

$$\ddot{\theta}_{b_2} = \ddot{\theta}_1 + \sum_{i=1}^{\infty} \varphi'_{1i}(L)\ddot{q}_{1i} + \ddot{\theta}_2 \tag{54}$$

Furthermore

$$\begin{aligned} \ddot{y}_{b2} &= \ddot{y}_{1e}\cos(\theta_2) \\ &= \Big(L_1\ddot{\theta}_1 + \sum_{i=1}^{\infty} \varphi_{1i}(L)\ddot{q}_{1i}\Big)\cos(\theta_2) \end{aligned} \tag{55}$$

Introducing these two accelrations into (50) we obtain the description for beam 2, ie. (4) or:

$$\begin{aligned} &\omega_{2i}^2 q_{2i} + 2\zeta_{2i}\omega_{2i}\dot{q}_{2i} + \ddot{q}_{2i} = \\ &\quad \sum_{j=1}^{n} \kappa_{2ij}^* \ddot{q}_{2j} + \alpha_{2i}^* \left[\ddot{\theta}_2 + \ddot{\theta}_{b1} + \sum_{j=1}^{n} \varphi'_{1j}(L_1)\ddot{q}_{1j}(t) \right] \\ &\quad + \beta_{2i}^* \left[L_1\ddot{\theta}_{b1} + \sum_{j=1}^{n} \varphi_{1j}(L_1)\ddot{q}_{1j} \right] \cos(\theta_2) \end{aligned}$$

F Equations of Motion in a Compact Form

If we define the vectors $\underline{q}_1$ and $\underline{q}_2$ as

$$\underline{q}_1 = \begin{bmatrix} q_{11} \\ \vdots \\ q_{1n} \end{bmatrix}, \quad \underline{q}_2 = \begin{bmatrix} q_{21} \\ \vdots \\ q_{2n} \end{bmatrix} \tag{56}$$

then the acturator equations (1) and (2) can be brought into a more compact form

$$\dot{\theta}_{b1} = P_1 u_1 + P_2 \underline{q}_1 \tag{57}$$

$$\dot{\theta}_2 = P_3 u_2 + P_4 \underline{q}_2 \tag{58}$$

where P_i, $i = 1 \sim 4$ are given directly from (1) and (2).

If we introduce the matrices

$$M_6 = \begin{bmatrix} P_2 & 0 \\ 0 & P_4 \end{bmatrix}, \quad M_7 = \begin{bmatrix} P_1 & 0 \\ 0 & P_3 \end{bmatrix} \tag{59}$$

then the actuator dynamics, (57) and (58), can in a compact form be written as

$$\underline{\dot{\theta}} = M_6 u + M_7 \underline{q} \tag{60}$$

The link equations (6) and (4) can also be expressed in a condensed form. Let us introduce the notation:

$$W_i = \begin{bmatrix} \omega_{i1}^2 & & 0 \\ & \ddots & \\ 0 & & \omega_{in}^2 \end{bmatrix} \quad R_i = \begin{bmatrix} 2\zeta_{i1}\omega_{i1} & & 0 \\ & \ddots & \\ 0 & & 2\zeta_{in}\omega_{in} \end{bmatrix} \quad i = 1,\ 2$$

If (57) and (58) are introduced in (6) and (4) (for $\ddot{\theta}_{b1}$ and $\ddot{\theta}_2$, then the upper link can be described by

$$\begin{aligned} W_1 \underline{q}_1 + R_1 \dot{\underline{q}}_1 + \ddot{\underline{q}}_1 &= B_{11} \ddot{\underline{q}}_1 + B_{12} \left[P_1 \dot{u}_1 + P_2 \dot{\underline{q}}_1 \right] \\ &+ B_{13} \ddot{\underline{q}}_1 + B_{14} \underline{q}_2 + B_{15} \left[P_1 \dot{u}_1 + P_2 \dot{\underline{q}}_1 \right] + B_{16} \ddot{\underline{q}}_1 \\ &+ B_{17} u_2 + B_{18} \left[P_3 u_2 + P_4 \underline{q}_2 \right] \end{aligned} \tag{61}$$

where B_{1i}, $i = 1 \sim 8$ are defined through (6). Due to (37) B_{15} and B_{16} are affine in the pay load mass m_p. This can also be expressed as:

$$\begin{aligned} W_1 \underline{q}_1 + R_1 \dot{\underline{q}}_1 + \ddot{\underline{q}}_1 &= \left[B_{14} + B_{18} P_4 \right] \underline{q}_2 \\ &+ \left[B_{12} P_2 + B_{15} P_2 \right] \dot{\underline{q}}_1 + \left[B_{11} + B_{13} + B_{16} \right] \ddot{\underline{q}}_1 \\ &+ \left[B_{17} + B_{18} P_3 \right] u_2 + \left[B_{12} P_1 + B_{15} P_1 \right] \dot{u}_1 \\ &= P_{11} \underline{q}_2 + P_{12} \dot{\underline{q}}_1 + P_{13} \ddot{\underline{q}}_1 + P_{14} u_2 + P_{15} \dot{u}_1 \end{aligned} \tag{62}$$

where the latter equality implicitly defines P_{1i}, $i = 1 \sim 5$. That results in an affinity of m_p in P_{12}, P_{13} and P_{15}.

For the second link (or the lower arm) we can in a similar fashion express (4) as

$$\begin{aligned} W_2 \underline{q}_2 + R_2 \dot{\underline{q}}_2 + \ddot{\underline{q}}_2 &= B_{21} \ddot{\underline{q}}_2 \\ &+ B_{22} \left[P_3 \dot{u}_2 + P_4 \dot{\underline{q}}_2 + P_1 \dot{u}_1 + P_2 \dot{\underline{q}}_1 + B_{23} \ddot{\underline{q}}_1 \right] \\ &+ B_{24} \left[P_1 \dot{u}_1 + P_2 \dot{\underline{q}}_1 \right] + B_{25} \ddot{\underline{q}}_1 \end{aligned} \tag{63}$$

Here the affine dependency enters through B_{21}, B_{22} and B_{24}. An rearangement of this equation yields

$$\begin{aligned} W_2\underline{q}_2 + R_2\dot{\underline{q}}_2 + \ddot{\underline{q}}_2 &= B_{22}P_4\dot{\underline{q}}_2 + [B_{22}P_2 + B_{24}P_2]\,\dot{\underline{q}}_1 \\ &+B_{21}\ddot{\underline{q}}_2 + [B_{22}B_{23} + B_{25}]\,\ddot{\underline{q}}_1 + B_{22}P_3\dot{u}_2 \\ &+ [B_{22}P_1 + B_{24}P_1]\,\dot{u}_1 \\ &= P_{21}\dot{\underline{q}}_2 + P_{22}\dot{\underline{q}}_1 + P_{23}\ddot{\underline{q}}_2 + P_{24}\ddot{\underline{q}}_1 + P_{25}\dot{u}_2 + P_{26}\dot{u}_1 \end{aligned} \tag{64}$$

where, again, the latter equality implicitly defines the P_{2i} $i = 1 \sim 6$, which all are affine in m_p.

If we furthermore define

$$\underline{q} = \begin{bmatrix} \underline{q}_1 \\ \underline{q}_2 \end{bmatrix}, \quad u = \begin{bmatrix} u_1 \\ u_2 \end{bmatrix}, \quad \underline{\theta} = \begin{bmatrix} \theta_{b1} \\ \theta_2 \end{bmatrix}$$

the we can bring the description of the flexibility into the form

$$\ddot{\underline{q}} \;=\; M_1\underline{q} + M_2\dot{\underline{q}} + M_3\ddot{\underline{q}} + M_4\underline{u} + M_5\dot{\underline{u}} \tag{65}$$

where

$$\begin{aligned} M_1 &= \begin{bmatrix} -W_1 & P_{11} \\ 0 & -W_2 \end{bmatrix} \\ M_2 &= \begin{bmatrix} P_{12} - R_1 & 0 \\ P_{22} & P_{21} - R_2 \end{bmatrix} \\ M_3 &= \begin{bmatrix} P_{13} & 0 \\ P_{24} & P_{23} \end{bmatrix} \\ M_4 &= \begin{bmatrix} 0 & P_{14} \\ 0 & 0 \end{bmatrix} \\ M_5 &= \begin{bmatrix} P_{15} & 0 \\ P_{26} & P_{25} \end{bmatrix} \end{aligned}$$

The matrices, M_2, M_3 and M_5, are all affine in m_p.

G The frequency equation

The solution to the frequency equation

$$\cosh(x)\cos(x) = -1$$

or

$$\cos(x) = -\frac{1}{\cosh(x)}$$

(as illustrated in Figure 18) can numerically be found as the roots to

$$f(x) = \cos(x) + \frac{1}{\cosh(x)}$$

by means of eg. Newton-Rahpson iterations, ie.

$$x_{n+1} = x_n - \frac{f(x_n)}{f'(x_n)}$$

In Figure 18 the two terms are plotted and it is obvious that the last term vanish as x increases.

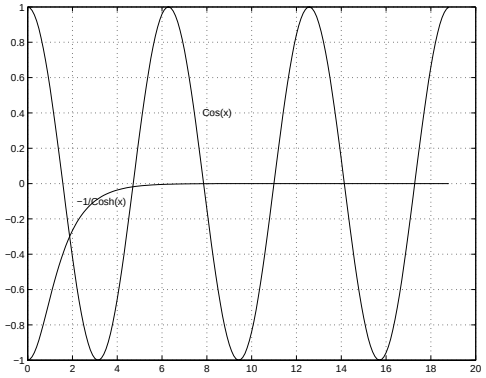

Figure 18. *Plot of the two terms in the frequency equation*

As pointed out in (Rostgaard 1995), the roots for $\cos(x)$, ie. $(i - \frac{1}{2})\pi$ is a good approximation (especially for large values of x) and a good starting point for the iterations.

```
function y=freqeq(n)
% Solves the frequency equation
%
% Cos(x)*Cosh(x)=-1
%
% for the first n solutions.

res=1e-5;

y=zeros(n,1);
for i=1:n,
 err=10;
 x=(i-0.5)*pi;
 while err>res,
  fx=cos(x)+1/cosh(x);
  dfx=-sin(x)-sinh(x)/cosh(x)^2;
  err=abs(fx);
  x=x-fx/dfx;
 end
 y(i)=x;
end
```

H Beam parameters

We are interesting in determine the beam constants in (45) and (44). For convenience we omit the i index in the following.

If

$$\mathbf{v}(x) = \begin{bmatrix} \cosh(\gamma x) \\ \sinh(\gamma x) \\ \cos(\gamma x) \\ \sin(\gamma x) \end{bmatrix}$$

then

$$\varphi(x) = \mathbf{c}\mathbf{v}(x)$$

where

$$\mathbf{c} = \begin{bmatrix} c_1 & c_2 & c_3 & c_4 \end{bmatrix}$$

From (Rottmann 1960) p. 146 we have

$$\begin{aligned} \int \cosh(\gamma x)dx &= \frac{1}{\gamma}\sinh(\gamma x) \\ \int \sinh(\gamma x)dx &= \frac{1}{\gamma}\cosh(\gamma x) \\ \int \cos(\gamma x)dx &= \frac{1}{\gamma}\sin(\gamma x) \\ \int \sin(\gamma x)dx &= -\frac{1}{\gamma}\cos(\gamma x) \end{aligned}$$

or

$$\int_0^L \mathbf{v}(x)dx = \tilde{A}\frac{1}{\gamma}\left(\mathbf{v}(L) - \mathbf{v}(0)\right)$$

where

$$\tilde{A} = \begin{bmatrix} 0 & 1 & 0 & 0 \\ 1 & 0 & 0 & 0 \\ 0 & 0 & 0 & 1 \\ 0 & 0 & -1 & 0 \end{bmatrix}$$

ie.

$$\beta = -\frac{4}{L}\int_0^L \varphi(x)dx = -4\mathbf{c}\tilde{A}\frac{1}{\gamma L}\left(\mathbf{v}(L) - \mathbf{v}(0)\right)$$

From (Rottmann 1960) we also have:

$$\begin{aligned} \int x\cosh(\gamma x)dx &= -\frac{1}{\gamma^2}\cosh(\gamma x) + \frac{x}{\gamma}\sinh(\gamma x) \\ \int x\sinh(\gamma x)dx &= -\frac{1}{\gamma^2}\sinh(\gamma x) + \frac{x}{\gamma}\cosh(\gamma x) \\ \int x\cos(\gamma x)dx &= \frac{1}{\gamma^2}\cos(\gamma x) + \frac{x}{\gamma}\sin(\gamma x) \\ \int x\sin(\gamma x)dx &= \frac{1}{\gamma^2}\sin(\gamma x) - \frac{x}{\gamma}\cos(\gamma x) \end{aligned}$$

or

$$\int_0^L x\mathbf{v}(x)dx = -\frac{1}{\gamma^2}\tilde{A}^2(\mathbf{v}(L) - \mathbf{v}(0)) + \frac{L}{\gamma}\tilde{A}\mathbf{v}(L)$$

ie.

$$\frac{\alpha}{L} = -\frac{4}{L}\int_0^L x\varphi(x)dx = \frac{4\mathbf{c}}{(\gamma L)^2}\tilde{A}^2\left(\mathbf{v}(L) - \mathbf{v}(0)\right) - \frac{4\mathbf{c}}{\gamma L}\tilde{A}\mathbf{v}(L)$$

```
function [gl,c,alfl,beta]=beamc(n)
%Usage: [gl,c,alfl,beta]=beamc(n)
%
%Determine the beam constants
%
% gl:   gamma_i*L
% c:    [c_{1i}, c_{2i}, c_{3i}, c_{4i}
% beta  beta_i
% alfl: alfa/L
%
% for i=1:n.

gl=freqeq(n); % gamma*L

iA=[0 1 0 0; 1 0 0 0; 0 0 0 1; 0 0 -1 0]; % iA=inv(A)

c=zeros(n,4);
beta=zeros(n,1);
alfl=zeros(n,1); % alfa/L
for i=1:n,
 ci=[0.5 -0.5*(cosh(gl(i))+cos(gl(i)))/(sinh(gl(i))+sin(gl(i)))];
 ci=[ci -ci];
 c(i,:)=ci;
 beta(i)=-4*ci*iA*(vfi(gl(i))-vfi(0))/gl(i);
 alfl(i)=ci*4*iA^2*(vfi(gl(i))-vfi(0))/gl(i)^2-4*ci*iA*vfi(gl(i))/gl(i);
end

function res=vfi(x)
res=[cosh(x);
     sinh(x);
     cos(x);
     sin(x) ];
```

References

Baungaard, J. R. (1996), Modelling and Control Flexible Robot Links, PhD thesis, Department of Automation, The Technical University of Denmark.

Kruise, L. (1990), Modelling and Control of a Flexible Beam and Robot Arm, PhD thesis, Universiteit Twente.

Leth, N. (1982), *Servomekanismer*, Servolaboratoriet.

Luca, A. D. & Panzieri, S. (1994), 'An iterative scheme for learning gravity compensation in flexible robot arms', *Automatica* **30**(6), 993–1002. Also as 12th World Congress of IFAC (1993), vol. 8, 191-198.

Middleton, R. & Goodwin, G. (1990), *Digital Control and Estimation, – a Unified Approach*, Prentice Hall.

M'Saad, M., Dugard, L. & Hammad, S. (1993), 'A suitable generalized predictive adaptive controller case study of a flexible arm', *Automatica* **29**(3), 589–608.

Parkum, J. E. (1992), Recursive Identification of Time-Varying Systems, PhD thesis, IMSOR buil. 321, Technical University of Denmark. IMSOR No. 57/92.

Rostgaard, M. (1995), Modelling, Estimation and Control of Fast Sampled Dynamical Systems, PhD thesis, IMM buil. 321, Technical University of Denmark.

Rottmann, K. (1960), *Matematishe formelsammlung*, Bibliographishes Institut.

Sakawa, Y., Matsuno, F. & Fukushima, S. (1985), 'Modelling and control of a flexible arm', *Journal of Robotic Systems* **2**, 453–472.

Timoshenko, S., Young, D. H. & Weaver, J. W. (1974), *Vibration Problems in Engineering*, John Wiley and Sons.